Electronic Supplementary Material (ESI) for Journal of Materials Chemistry A.
This journal is © The Royal Society of Chemistry 2018

Supporting Information for

Engineered Sub-100 nm $Mo_{(1-x)}W_xSe_2$ Crystals for Efficient Hydrogen Evolution Catalysis

Minghao Zhuang[1], Li-Yong Gan[2]*, Mingchu Zou[3], Yubing Dou[1], Xuewu Ou[1], Zhenjing Liu[1], Yao Ding[1], Irfan Haider Abidi[1], Abhishek Tyagi[1], Mahsa Jalali[1], Jiawen You[1], Anyuan Cao[3] and Zhengtang Luo[1]*

[1]*Department of Chemical and Biological Engineering, Hong Kong University of Science and Technology, Clear Water Bay, Kowloon, Hong Kong, 999077, China*

[2]*School of Materials Science and Engineering, Key Laboratory of Advanced Energy Storage Materials of Guangdong Province, South China University of Technology, Guangzhou 510641, China*

[3]*Department of Materials Science and Engineering, College of Engineering, Peking University, Beijing, 100871, China*

E-mail: ganly@scut.edu.cn, keztluo@ust.hk

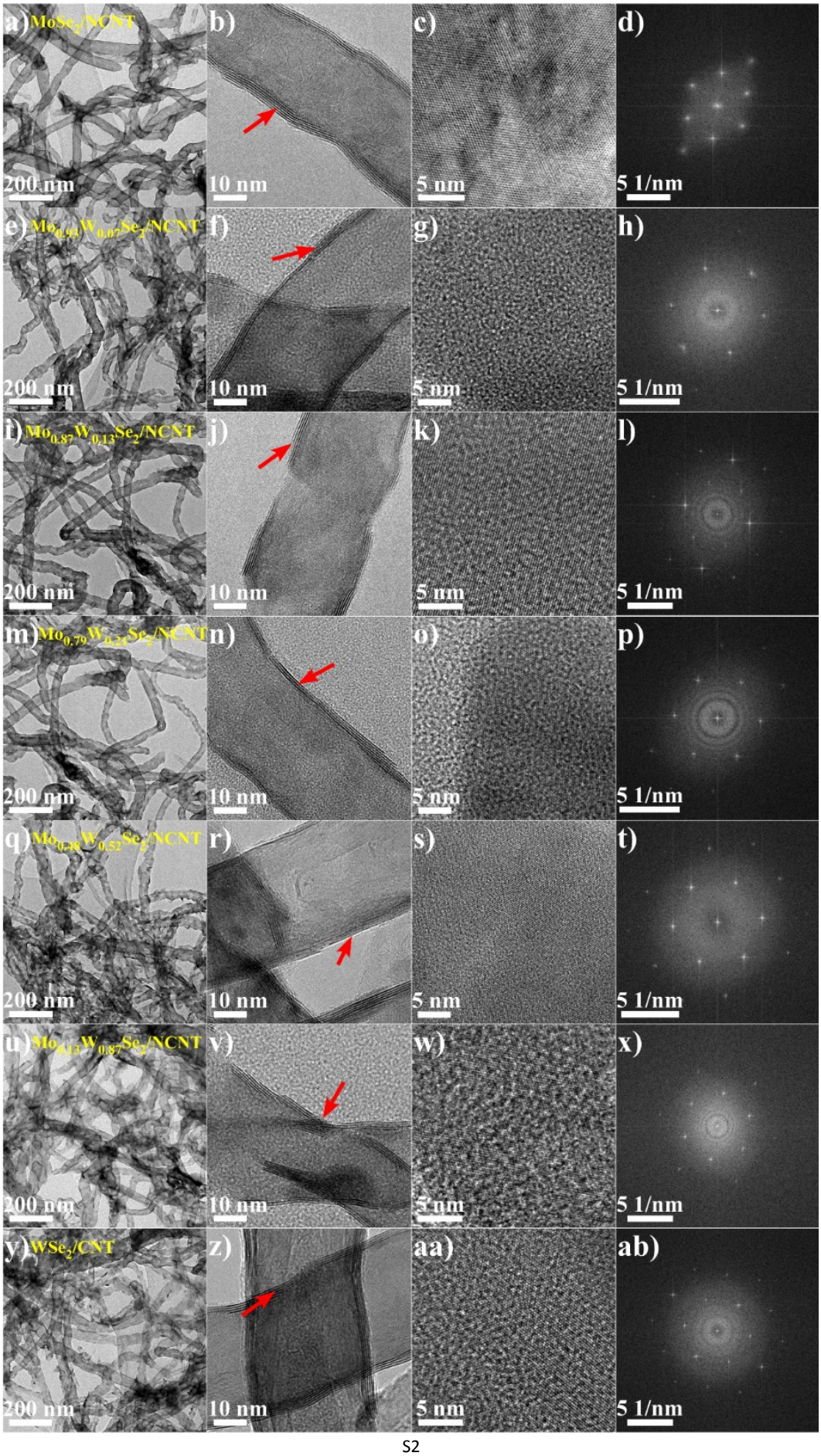
a) $MoSe_2$/NCNT
b)
c)
d)
200 nm
10 nm
5 nm
5 1/nm
e) $Mo_{0.93}W_{0.07}Se_2$/NCNT
f)
g)
h)
200 nm
10 nm
5 nm
5 1/nm
i) $Mo_{0.87}W_{0.13}Se_2$/NCNT
j)
k)
l)
200 nm
10 nm
5 nm
5 1/nm
m) $Mo_{0.79}W_{0.21}Se_2$/NCNT
n)
o)
p)
200 nm
10 nm
5 nm
5 1/nm
q) $Mo_{0.48}W_{0.52}Se_2$/NCNT
r)
s)
t)
200 nm
10 nm
5 nm
5 1/nm
u) $Mo_{0.12}W_{0.87}Se_2$/NCNT
v)
w)
x)
200 nm
10 nm
5 nm
5 1/nm
y) WSe_2/CNT
z)
aa)
ab)
200 nm
10 nm
5 nm
5 1/nm

Figure S1. TEM results of $Mo_{(1-x)}W_xSe_2$ crystals on MWCNT. a, e, i, m, q, u, y) Low-resolution TEM image of $Mo_{(1-x)}W_xSe_2$ nanocrystals on MWCNT with x of 0, 0.07, 0.13, 0.21, 0.52, 0.87 and 1, respectively. **b, f, j, n, r, v, z)** corresponding close-up TEM images of $Mo_{(1-x)}W_xSe_2$ nanocrystals grown on MWCNT. The nanocrystals are pointed out by red arrows. **c, g, k, o, s, w, aa)** High-resolution TEM (HRTEM) images of the basal plane of corresponding $Mo_{(1-x)}W_xSe_2$ nanocrystals. **d, h, l, p, t, x, ab)** the FFT pattern of single-crystalline $Mo_{(1-x)}W_xSe_2$ nanocrystals.

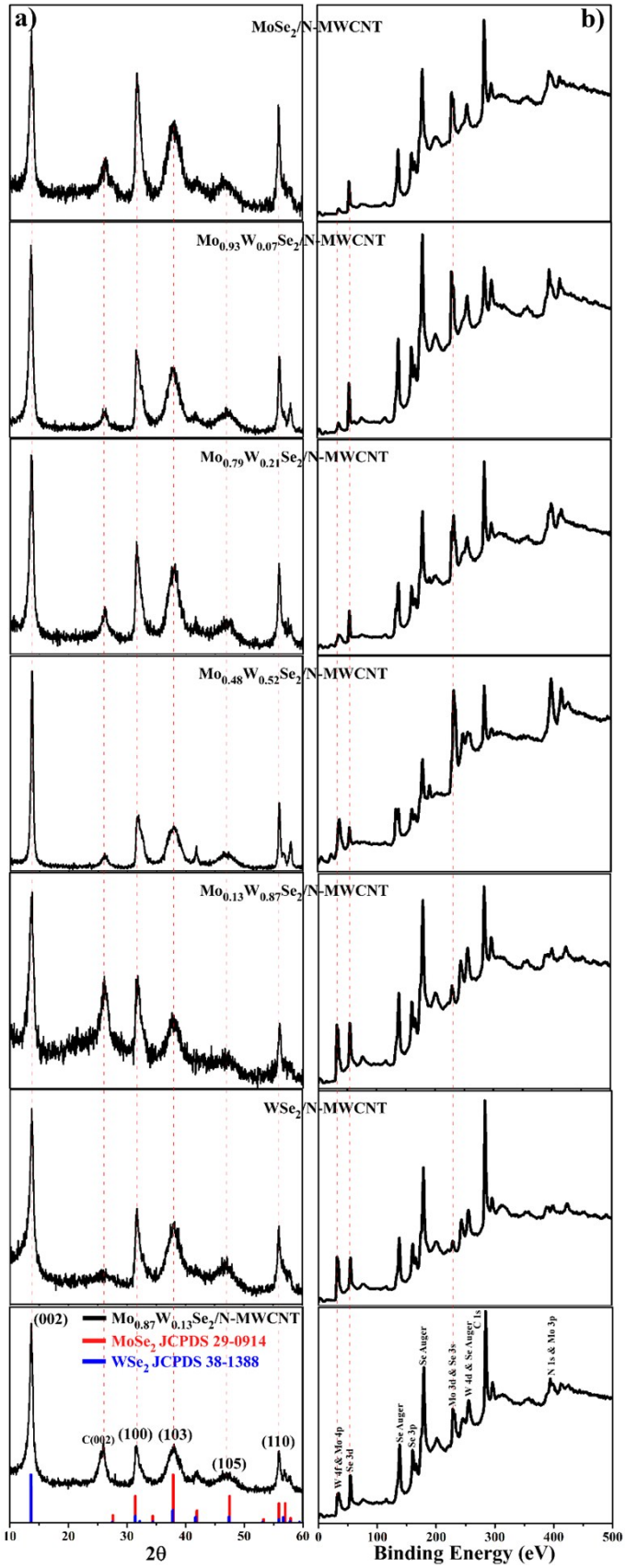

Figure S2. a) XRD and b) XPS spectra of $Mo_{(1-x)}W_xSe_2$/N-MWCNT with various W composition x from 0 to 1.

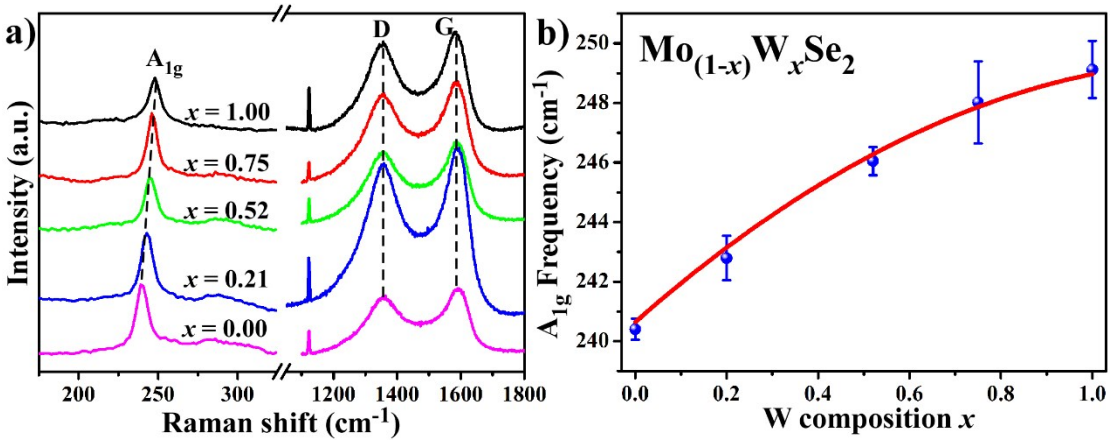

Figure S3. Raman spectra of $Mo_{(1-x)}W_xSe_2$/N-MWCNT with various W composition *x*. a) Raman spectra of $Mo_{(1-x)}W_xSe_2$/N-MWCNT with *x* from 0 to 1. The A_{1g} peak shift is guided by dotted line, while the D and G peaks of reduced graphene oxide keep at the same position. **b)** Plots of A_{1g} frequencies versus W composition *x*, the blue dots represent experimental data and the red line as the fitting trend. The excitation laser wavelength is 514 nm and all the spectra are calibrated with the 520 cm^{-1} Raman peak from pure SiO_2/Si substrate.

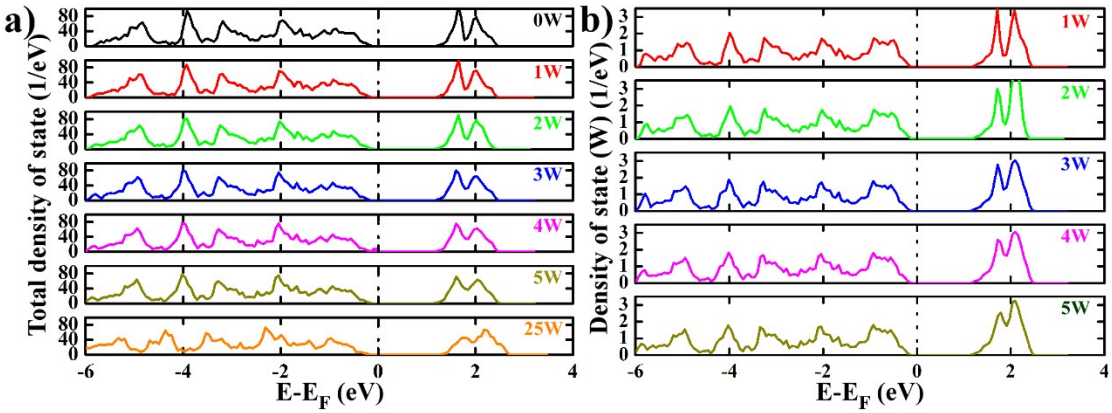

Figure S4. Density of state results of $Mo_{(1-x)}W_xSe_2$ with various number of W atom doping. a) Total density of state results of crystals with different W concentration. **b)** The independent density of state curves of W atom in all crystals.

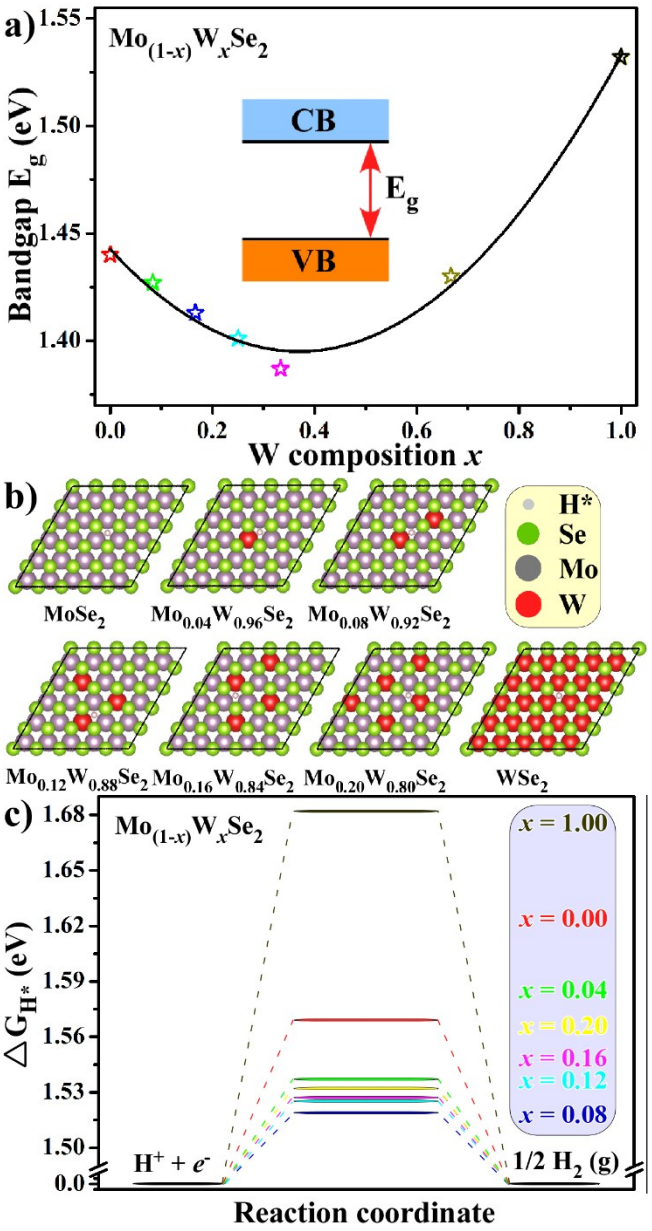

Figure S5. Density Functional Theory (DFT) calculation results. a) Bandgap E_g values of $Mo_{(1-x)}W_xSe_2$ crystals as a function of x. **b)** Structural models of $Mo_{(1-x)}W_xSe_2$ crystals with the adsorbed hydrogen atoms. The grey, red, green and white spheres represent Mo, W, Se and the adsorbed hydrogen atoms, respectively. **c)** Calculated Gibbs free energy diagram for HER on $Mo_{(1-x)}W_xSe_2$ basal planes with W composition x from 0 to 1.

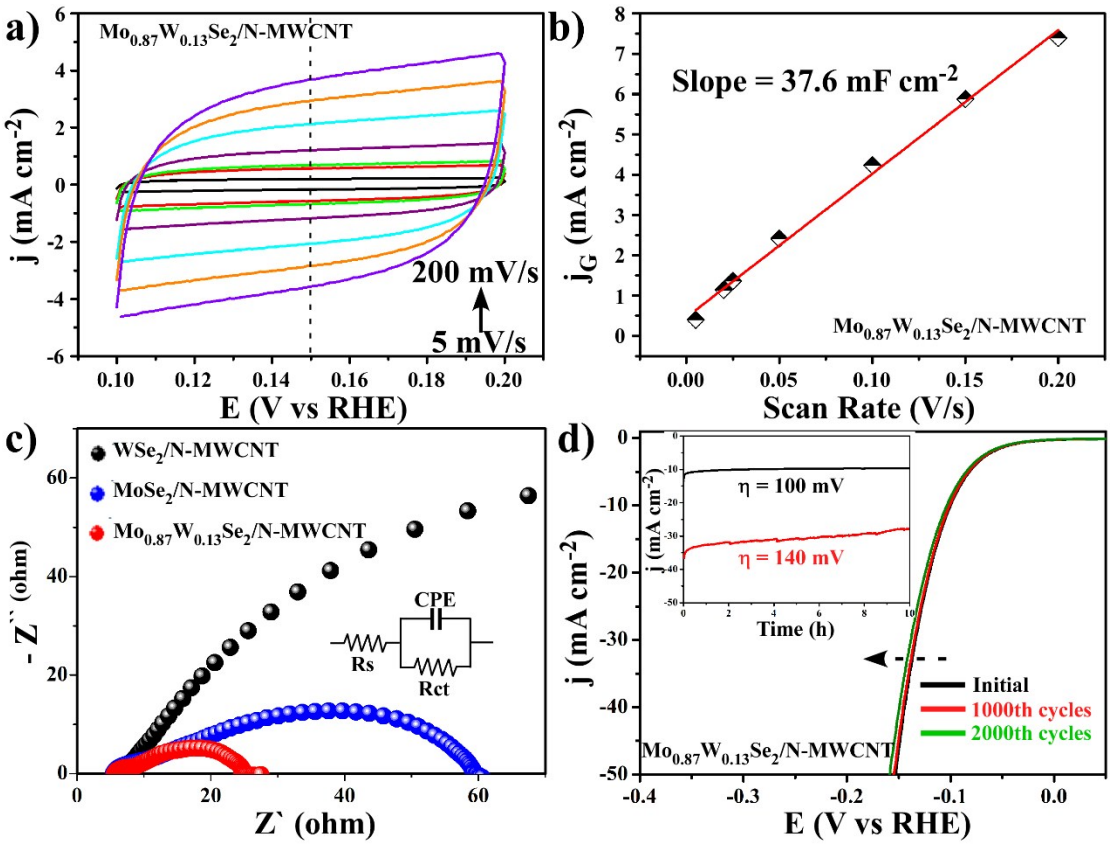

Figure S6. Electrochemical properties of $Mo_{0.87}W_{0.13}Se_2$/N-MWCNT catalyst. a) Cyclic voltammograms within the range of non-faradaic reactions. **b)** Variation of double-layer charging currents at 0.15 V as a function of voltage scan rate. Symbols and solid line are experimental data from c and the linear fitting. **c)** Nyquist plots of various catalysts loaded electrodes at the overpotential of 150 mV. **d)** Polarization curves of $Mo_{0.87}W_{0.13}Se_2$/N-MWCNT after 1000 and 2000 cycles. Inset is the time dependence of cathodic current density during electrolysis at the overpotentials of 100 mV and 140 mV, respectively. *Noted here the $Mo_{0.87}W_{0.13}Se_2$/N-MWCNT mass loading in d) is 2 mg cm^{-2}, more than the loading applied in array comparison, however it still exhibited high durability in long term testing, indicating that the $Mo_{0.87}W_{0.13}Se_2$/N-MWCNT could be promising in practical applications.*

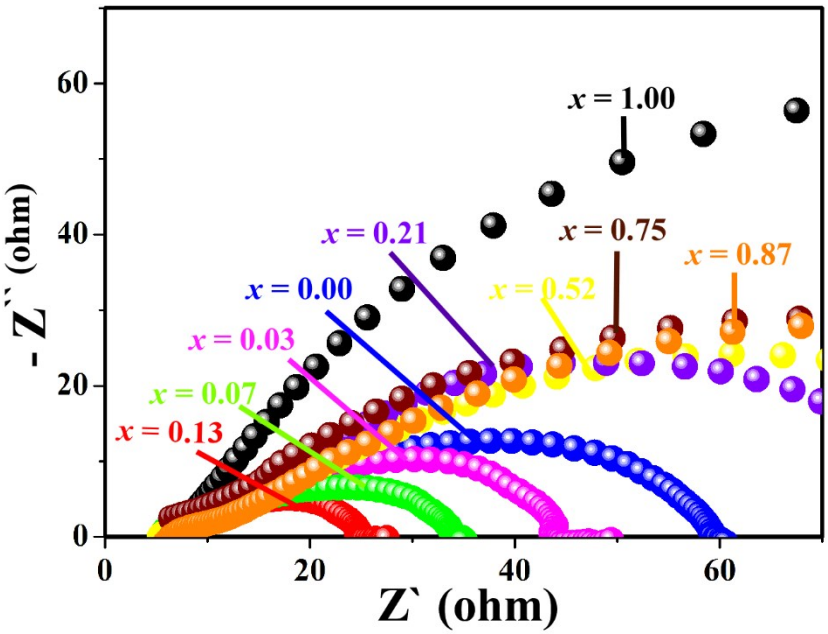

Figure S7. Nyquist plots of $Mo_{(1-x)}W_xSe_2$/N-MWCNT catalysts loaded electrodes at the overpotential of 150 mV with different *x* from 0 to 1 in the same condition.

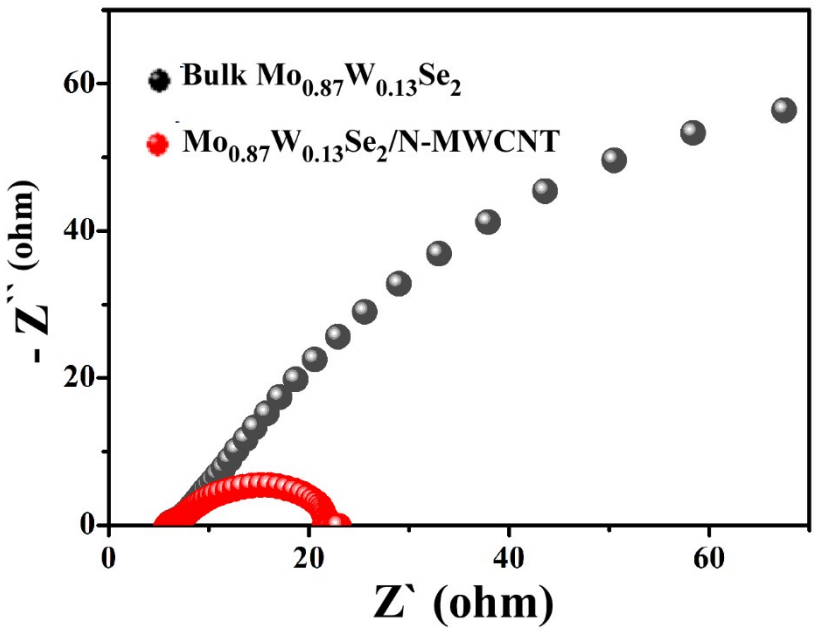

Figure S8. Nyquist plots of bulk $Mo_{0.87}W_{0.13}Se_2$ and $Mo_{0.87}W_{0.13}Se_2$/N-MWCNT catalysts loaded electrodes at the overpotential of 150 mV in the same condition.

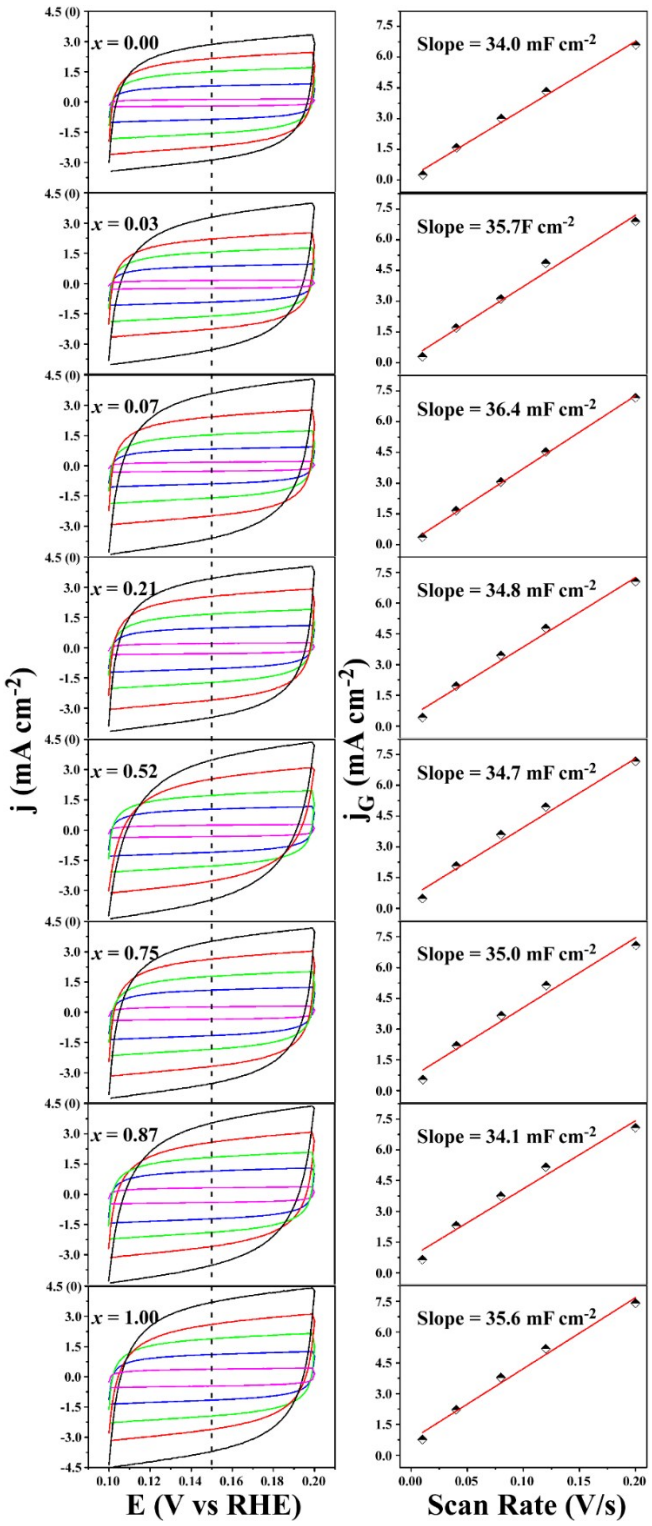

Figure S9. Cyclic voltammograms (CV) wthin the range of non-faradaic reactions of $Mo_{(1-x)}W_xSe_2$/N-MWCNT with various W composition *x*, scan rate is from 5 to 200 mV, and corresponding variation of double-layer charging currents at 0.15 V as a function of voltage scan rate. Symbols and solid lines are experimental data and linear fitting, respectively.

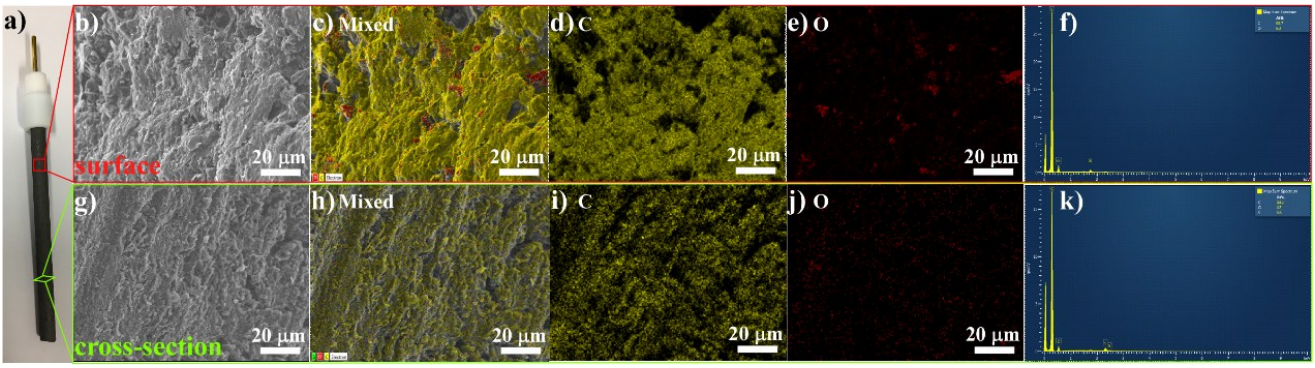

Figure S10. SEM images and EDS mapping results of carbon bar (counter electrode). a) photograph of carbon bar used as counter electrode in this work. **b)** SEM image of the carbon bar surface. Followed by **c)** mixed elemental mapping, **d)** carbon elemental mapping, **e)** oxygen elemental mapping and **f)** elemental percentage spectrum of the surface of carbon bar, C atom% is 93.7% and O atom% is 6.3%. **g)** SEM image of the cross-section of carbon bar. Followed by **h)** mixed elemental mapping, **i)** carbon elemental mapping, **j)** oxygen elemental mapping and **k)** elemental percentage spectrum of the cross-section of carbon bar, C atom% is 94.9%, O atom% is 4.5% and S atom% is 0.6%. There is no metal or other HER-active impurities in/on the carbon bar.

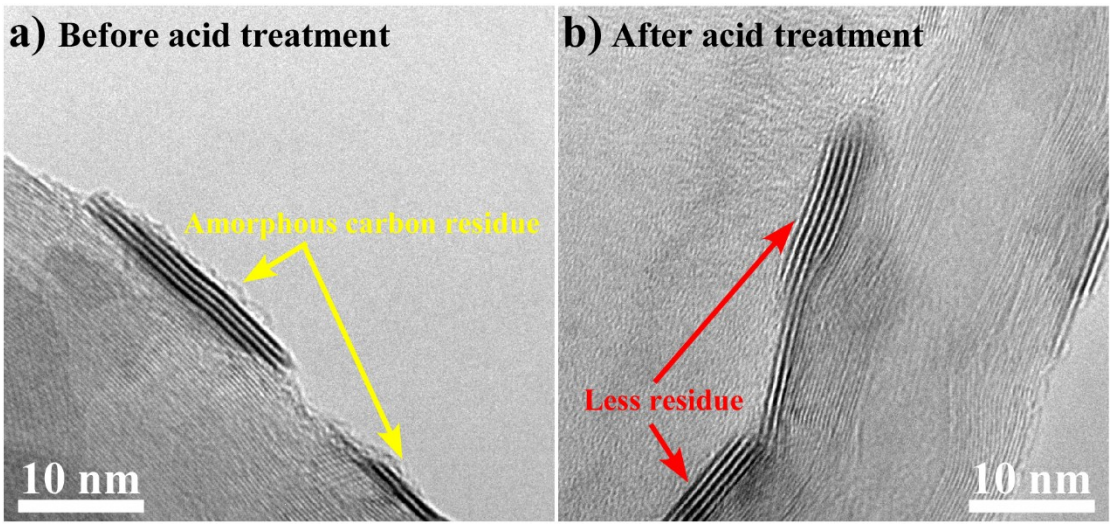

Figure S11. TEM images of $Mo_{(1-x)}W_xSe_2$/N-MWCNT before and after acid treatment. a) Before acid treatment, there is some amorphous carbon residues around crystal surface. **b)** After acid treatment, the carbon residues become less and the surface of crystal is more smooth and clean.

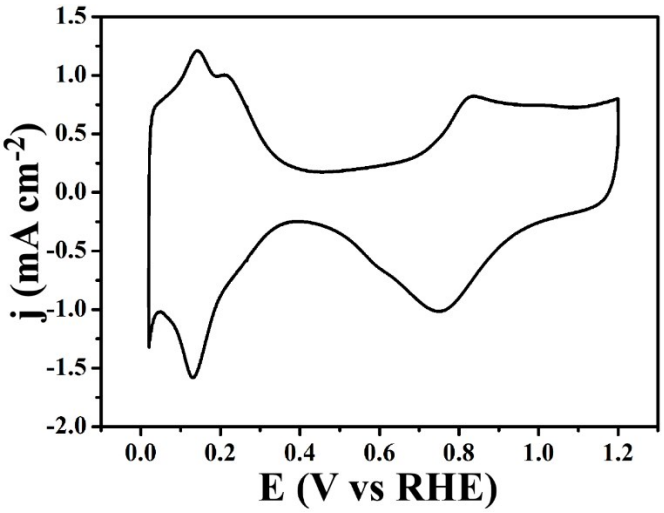

Figure S12. Fingerprint Cyclic Voltammetry Curve of Commercial Pt/C (46%, TEC10E50E, TKK) in Ar-saturated 0.1 M $HClO_4$ at a scan rate of 50 mV s^{-1}. For commercial Pt/C electrode preparation, 10 mg of Pt/C powder was ultrasonically dispersed in 5 mL of a 4:1 (v:v) water/2-propanol mixed solvents along with 20 μL of Nafion solution for 15 min. 20 μL of above suspension was deposited on a polished and clean glassy carbon (d = 5 mm) and dry naturally in the air for testing (mass loading is 0.2 mg cm^{-2}). The calculated electrochemical surface area (ECSA) is ~60 m^2/g_{Pt}.

Table S1. Recently reported Mo/W-based TMDs electrocatalysts towards hydrogen evolution reaction (HER) in 0.5 M H_2SO_4							
Catalyst	***Synthesis Method***	***Mass Loading (mg cm^{-2})***	***Current Density j (mA cm^{-1})***	***Overpotential at j (mV)***	***Tafel Slope (mV dec^{-1})***	***Exchange Current Density (μA cm^{-2})***	***Ref.***
$Mo_{0.87}W_{0.13}Se_2$/N-	Wet-chemical combined	0.2	-10	129	53.6	49.5	Our work

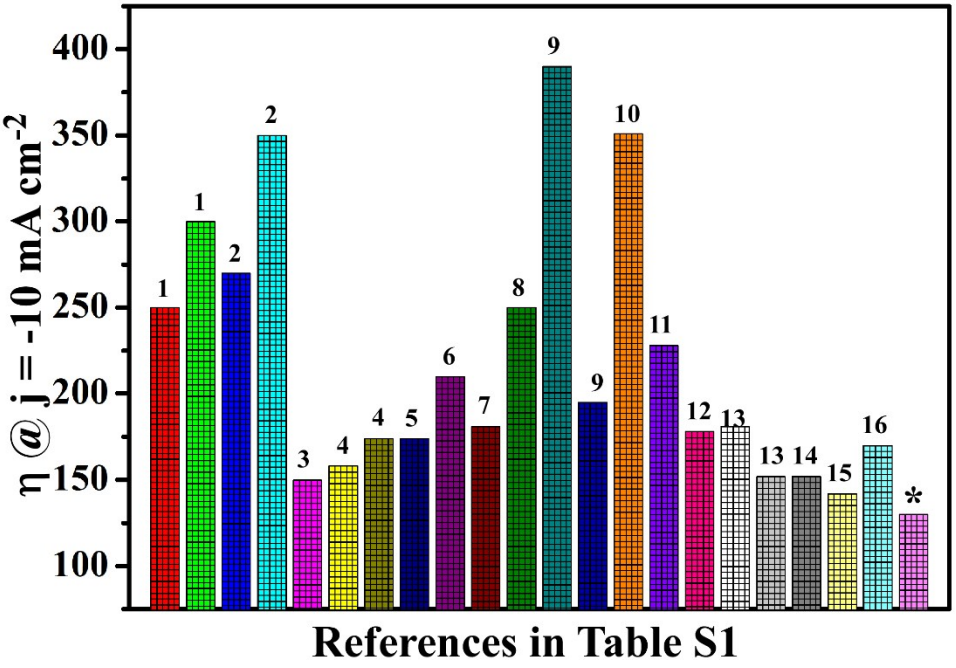

Figure S13. Comparison of overpotentials needed to achieve the geometric current density of -10 mA cm^{-2} in Table S1. The details of references are as following: **1.** Nano Lett. 2013, 13, 3426; **2.** ACS Nano, 2014, 8, 8468; **3.** Adv. Mater. 2015, 27, 4732; **4.** J. Mater. Chem. A, 2015, 3, 18090; **5.** J. Mater. Chem. A, 2015, 3, 16263; **6.** Chem. Mater. 2016, 28, 1838; **7.** Adv. Funct. Mater. 2016, 26, 8537; **8.** ACS Catal., 2014, 4, 2866; **9.** J. Mater. Chem. A, 2015, 3, 19706; **10.** Nanoscale, 2015, 7, 18595; **11.** J. Mater. Chem. A, 2015, 3, 12149; **12.** Nanoscale, 2015, 7, 18595; **13.** Nanoscale, 2016, 8, 15262; **14.** J. Am. Chem. Soc., 2011, 133, 7296; **15.** Energy Environ. Sci., 2014, 7, 2608; **16.** Nat. Mater., 2016, 15, 48. **Noted that * is our work.**

$MoSe_2$ on carbon fiber paper	CVD (vertical sheets)	-	-10	250	59.8	0.38	Nano Lett. 2013, 13, 3426
WSe_2 on carbon fiber paper				300	77.4	-	
$WS_{2(1-x)}Se_{2x}$ NTs	CVD	~0.21	-10	~270	105	29	ACS Nano, 2014, 8, 8468
WSe_2				~350	99	3	
$WS_{2(1-x)}Se_{2x}$ monolayer	CVD	-	-10	150	85	-	Adv. Mater. 2015, 27, 4732
WSe_2-C-20	CVD (triangular)	-	-10	158	98	240	J. Mater. Chem. A, 2015, 3, 18090
$W(Se_{0.4}S_{0.6})_2$-C-10				174	106	229	
$MoSe_2$ microspheres	colloidal route	-	-5	100	56	-	Nano Res. 2015, 8, 1108
rGO/PI–MoSe 2 nanoparticles $MoSe_2$–rGO/PI composite	electrodeposition	-	-4.9	100	82	-	Adv. Funct. Mater. 2015, 25, 1814
			-7.9	200			
SnO_2@$MoSe_2$	solvothermal	-	-10	~174	51		J. Mater. Chem. A, 2015, 3, 16263
$MoSe_2$−NiSe	solvothermal	~0.285	-10	210	56	-	Chem. Mater. 2016, 28, 1838
MoO_2/$MoSe_2$ Core–Shell Nanosheet	CVD	~0.13	-10	181	49.1	1.36	Adv. Funct. Mater. 2016, 26, 8537
$MoSe_2$ (Macroporous)	wet-chemical	1.36 mg cm^{-2}	-10	250	80	0.01	ACS Catal., 2014, 4, 2866
$MoSe_2$	solvothermal	0.285	-10	390	103	-	J. Mater. Chem. A, 2015, 3, 19706
$MoSe_2$/graphene				195	67		

PhLi-$MoSe_2$	Aromatic - Exfoliated	-	-10	351	54	-	ACS Catal. 2016, 6, 4594
WSe_2/CFM 3D carbon nanofiber mats	CVD (dendritic)	2.2	-10	228	80	15	J. Mater. Chem. A, 2015, 3, 12149
CNT@ $MoSe_2$	solvothermal	-	-10	178	58	-	Nanoscale, 2015, 7, 18595
MoS_2	colloidal	0.43	-10	181	52	-	Nanoscale, 2016, 8, 15262
WS_2				152	46		
MoS_2/RGO	solvothermal	0.28	-10	~152	41	-	J. Am. Chem. Soc., 2011, 133, 7296
WS_2 nanosheets	CVD	1.0	-10	142	70	93	Energy Environ. Sci., 2014, 7, 2608
Strained vacancy MoS_2	CVD	-	-10	170	60	-	Nat. Mater., 2016, 15, 48
Stepped edge surface-terminated MoS_2	Hydrothermal	3.2	-10	104	59	200	Energy Environ. Sci., 2017, 10, 593

Table S2. Structures and hydrogen adsorption energies (ΔE_{H^*} and ΔG_{H^*}) for $Mo_{(1-x)}W_xSe_2$. The grey, red, green and white spheres represent Mo, W, Se and the adsorbed hydrogen atoms, respectively.

$Mo_{(1-x)}W_xSe_2$	x	Stable structure	ΔE_{H^*} (eV)	ΔG_{H^*} (eV)
Basal plane	0%	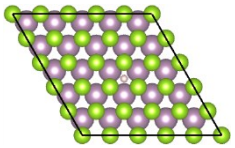	1.289	1.569
	4%	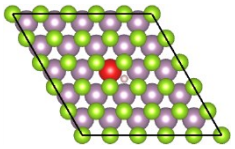	1.257	1.537
	8%	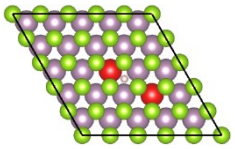	1.239	1.519
	12%	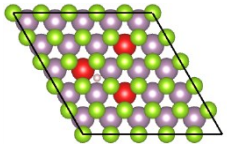	1.245	1.525
	16%	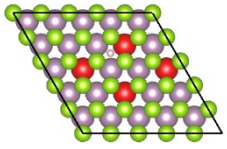	1.247	1.527
	20%	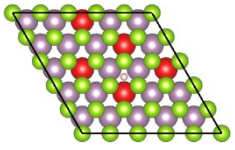	1.252	1.532
	100%	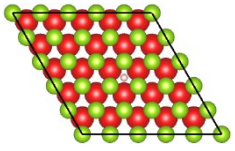	1.402	1.682
Edge	0%	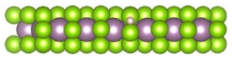	-0.861	-0.581
	2.38%	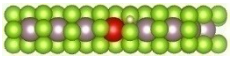	-0.407	-0.127
	2.38%	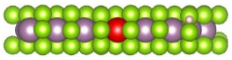	-0.663	-0.383
	4.76%	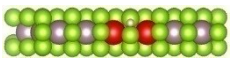	0.051	0.331
	4.76%	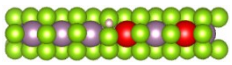	0.019	0.299

	7.14%	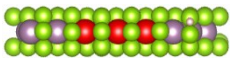	-0.874	-0.594
	7.14%	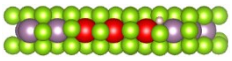	-0.361	-0.081
	7.14%	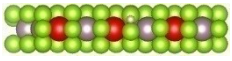	-0.736	-0.456
	14.29% (Mo-edge)	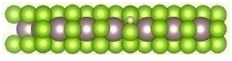	-0.933	-0.653
	14.29% (W-edge)	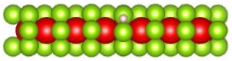	-0.450	-0.170